IOP Conf. Series: Materials Science and Engineering **158** (2016) 012004 doi:10.1088/1757-899X/158/1/012004

Numerical simulation of liquid jet impact on a rigid wall

A A Aganin and T S Guseva

Institute of Mechanics and Engineering, Kazan Science Center, Russian Academy of Sciences, 420111 Kazan, Russian Federation

E-mail: ts.guseva@mail.ru

Abstract. Basic points of a numerical technique for computing high-speed liquid jet impact on a rigid wall are presented. In the technique the flows of the liquid and the surrounding gas are governed by the equations of gas dynamics in the density, velocity, and pressure, which are integrated by the CIP-CUP method on dynamically adaptive grids without explicitly tracking the gas-liquid interface. The efficiency of the technique is demonstrated by the results of computing the problems of impact of the liquid cone and the liquid wedge on a wall in the mode with the shockwave touching the wall by its edge. Numerical solutions of these problems are compared with the analytical solution of the problem of impact of the plane liquid flow on a wall. Applicability of the technique to the problems of the high-speed liquid jet impact on a wall is illustrated by the results of computing a problem of impact of a cylindrical liquid jet with the hemispherical end on a wall covered by a layer of the same liquid.

1. Introduction

The impact of high-speed liquid jets (or drops) on a wall is of considerable interest to applications as it can lead to the wall damages. Such problems can occur, for example, with aircrafts flying in a rain, with operating steam turbines [1, 2]. High-speed microjets directed to a wall can arise on the surface of cavitation bubbles at their non-spherical collapse near the wall. The impact of such jets is considered to be one possible cause of destruction of the surfaces of bodies operating in the conditions of cavitation [3, 4].

Important features of the high-speed jet impact on a wall are shockwaves which can arise in the liquid and the surrounding gas, the strong deformations of the liquid-gas interface. These features need to be allowed for while choosing a mathematical model as well as a numerical method, and they were taken into account in realizing the numerical technique of the present work.

2. Basic points of the numerical technique

The numerical technique is based on the approach without explicit separation of the interface. Similar to [5], an identifier-function φ is used to identify a fluid: $\varphi = 1$ in the liquid and $\varphi = 0$ in the gas. In a small vicinity of the gas-liquid interface the identifier φ is continuous and monotonically changing from 0 to 1. The identifier φ is governed by the advection equation

$$\varphi_t + \mathbf{u} \cdot \nabla\varphi = 0, \qquad (1)$$

where $\mathbf{u}$ is the advection velocity.

Dynamics of the liquid and the gas is computed by the CIP-CUP method [6]. It is based on equations of motion of a compressible medium in primitive variables (density, velocity, pressure), which allows one to perform calculation without explicit separation of the interface [7]. Without allowing for the effects of viscosity and heat conductivity those equations can be written in the form

$$\mathbf{f}_t + \mathbf{u}\cdot\nabla\mathbf{f} = \mathbf{G} \qquad (2)$$

where $\mathbf{f} = (\rho, \mathbf{u}, p)^T$, $\mathbf{G} = (-\rho\nabla\cdot\mathbf{u}, -\rho^{-1}\nabla p, -\rho C_S^2\nabla\cdot\mathbf{u})^T$, ρ is the density, p is the pressure, $C_S = \varphi C_{S1}+(1-\varphi)\, C_{S2}$ is the sound speed, $C_{Si} = [\Gamma_i(p+B_i)/\rho]^{1/2}$, $i = 1$ corresponds to the liquid, $i = 2$ to the gas, Γ_1, B_1 are the constants of the Tait equation of the liquid state, $\Gamma_2 = \gamma$, $B_2 = 0$, γ is the isentropic exponent of gas.

System (2) is numerically integrated by splitting into the advection and non-advection parts.

$$\frac{\mathbf{f}^* - \mathbf{f}^n}{\Delta t^n} + \mathbf{u}\cdot\nabla\mathbf{f} = 0\,, \qquad (3)$$

$$\frac{\mathbf{f}^{n+1} - \mathbf{f}^*}{\Delta t^n} = \mathbf{G}\,. \qquad (4)$$

Semi-Lagrangian method CIP (Constrained Interpolation Profile) [5] is applied to compute the group of advection equations (3). The solution of the advection equation for a function f at a grid point $\mathbf{x}$ at a time moment $t^{n+1} = t^n + \Delta t^n$ can be approximately written as $f(\mathbf{x}-\mathbf{u}\Delta t^n)$ where the argument is a departure point meaning the location of the "Lagrangian particle" which in time interval Δt^n will arrive at the grid point $\mathbf{x}$. The value of the function f at the departure point is determined by CIP-interpolation using known values of f and its spatial derivatives at the grid points at the moment t^n.

Non-advection part (4) is reduced to the following pressure equation

$$\frac{p^{n+1} - p^*}{\rho^* C_S^{*2} \Delta t^{n2}} = \nabla\cdot\left(\frac{\nabla p^{n+1}}{\rho^*}\right) - \frac{\nabla\cdot\mathbf{u}^*}{\Delta t^n}\,,$$

which is integrated by the well-known SOR method. Then $\mathbf{u}^{n+1}$ and ρ^{n+1} are calculated. In solving problems with strong shockwaves the CIP-CUP method is used in combination with the artificial viscosity.

Calculations are carried out with the use of dynamically adaptive grids [8]. In the two-dimensional case, the grid is a set of points located on parallel straight lines. At each time step a new grid adapted to the solution and independent of the old grid is constructed. In doing so, the number and the relative position of the grid lines and the grid points on those lines can change.

In creating a grid, a monitoring function $M(x, y, t)$ defined as

$$M(x,y,t) = \left(1+\alpha\left(f_x^{\,2} + f_y^{\,2}\right)\right)^{1/2} + \beta\left(\left|f_{xx}\right| + \left|f_{yy}\right|\right)$$

is first calculated. Here f is some parameter of the solution, α, β are some positive coefficients. The lines and the points of the grid are condensed in the zones with large values of the monitoring function and are rarefied where the values of the function are small. In the finite-difference approximations to the derivatives, the necessary values of the parameters at the points of the stencil are determined by CIP interpolation [8].

3. Impact of a liquid cone and a liquid wedge on a wall

To estimate the efficiency of a numerical technique of computing the jet impact on a solid surface it is possible to use a model problem of a liquid cone impact on a wall. For this purpose the case of impact of a liquid blunt cone on a plane wall is considered in the present paper (Fig. 1*a*). The slope of the cone surface to the wall is sufficiently small so that a shockwave with the edge attached to the wall is formed in the liquid. The circular area $r \le R_L$ ($R_L = V\,t \operatorname{ctg}\theta$, V is the impact velocity, θ is the angle of the slope of the cone surface, r is the distance to the axis of symmetry) of contact of the liquid and the wall quickly expands. The sideway spreading of the liquid on the wall does not arise.

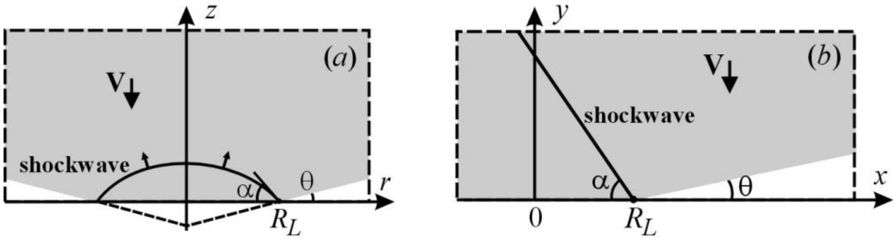

Figure 1. The schematic of the impact of a liquid blunt cone (*a*) and the plane semi-infinite liquid flux with the same slope of the boundary (*b*) on the horizontal fixed wall.

Following [9], we estimate the value of the pressure of the compressed liquid in the vicinity of the shockwave edge ($r \approx R_L$) in the problem of the liquid cone impact (Fig. 1*a*) by the value of the pressure of the everywhere-equally compressed liquid behind the shockwave in the problem of impact of a plane semi-infinite liquid flux with the same liquid velocity and the same slope of the flux boundary (Fig. 1*b*). In the latter problem, the pressure of the compressed liquid behind the shockwave is determined by

$$p = p_0 - \rho_{L0}\frac{V^2}{\sin^2\theta}\sin(\alpha+\theta)\left[\sin(\alpha+\theta)-\cos(\alpha+\theta)\,\mathrm{tg}\,\alpha\right], \quad (5)$$

where the shockwave slope angle α is found from the equation

$$\mathrm{tg}^3(\alpha+\theta)\left(\frac{\Gamma-1}{2}M_1^{\ 2}+1\right)-\theta\left(M_1^{\ 2}-1\right)\mathrm{tg}^2(\alpha+\theta)+\left(\frac{\Gamma+1}{2}M_1^{\ 2}+1\right)\mathrm{tg}(\alpha+\theta)+\mathrm{ctg}\,\theta=0\,.$$

Here Γ is the constant of the Tait equation of the liquid state, $M_1 = V/(C\sin\theta)$, p_0, ρ_{L0}, C are the pressure, the density, and the sound speed in the undisturbed liquid.

Some differences between the values of the pressure of the compressed liquid in the vicinity of the shockwave edge in the former problem and that behind the shockwave in the latter problem can be caused by the influence of the axial symmetry. To estimate this influence the numerical solution of the similar plane problem of the liquid wedge impact is utilized.

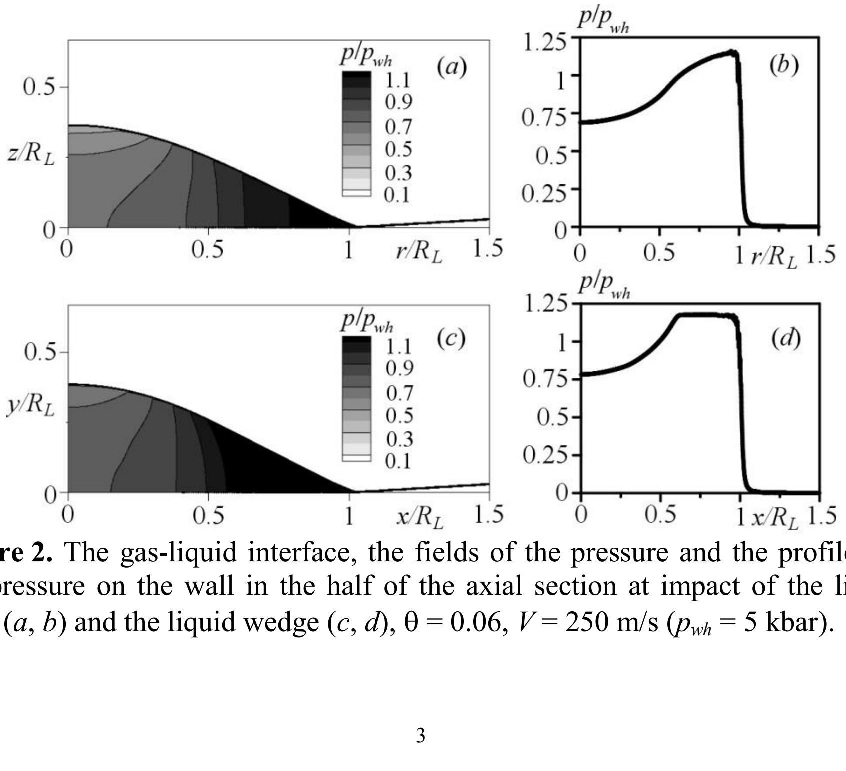

Figure 2. The gas-liquid interface, the fields of the pressure and the profiles of the pressure on the wall in the half of the axial section at impact of the liquid cone (*a*, *b*) and the liquid wedge (*c*, *d*), $\theta = 0.06$, $V = 250$ m/s ($p_{wh} = 5$ kbar).

Typical numerical results on impact of the liquid cone and the liquid wedge on the wall in case of small values of θ are illustrated in Fig. 2. The liquid ($\Gamma_1 = 7.15$, $B_1 = 3072$ bar) is assumed to be surrounded by a gas (γ=1.4). At the initial moment $\varphi = 1$, $\rho = 10^3$ kg/m^3 in the liquid, $\varphi = 0$, $\rho = 1$ kg/m^3 in the gas, and $p = 1$ bar everywhere. In Fig. 2 the pressure p is referred to the waterhammer pressure p_{wh}, which can be estimated approximately as $p_{wh} = \rho_{L0}DV$ where D is the shockwave velocity, $D \approx C + 2V$ for water [9]. One can see in Fig. 2 that the main features of the impact (the geometry of the shockwave front, the distribution and the maximum and minimum levels of the compressed liquid pressure) are almost infependent of the axial symmetry. At the same time, in the presence of the axial symmetry the distribution of the liquid pressure on the wall is everywhere nonuniform with the clear maximum at the imact area edge $r = R_L$, while in the absence of the axial symmetry this distibution has, near the imact area edge $x = R_L$, quite a large plateau at the level of the maximum pressure.

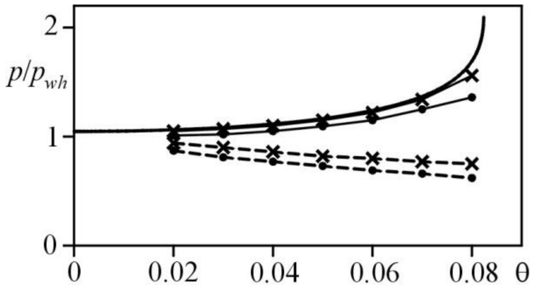

Figure 3. Dependences of the liquid pressure on the wall on the slope angle θ in the cases of impact by (i) the plane semi-infinite liquid flux (curve without symbols, calculated by (5)), (ii) the liquid cone (curves with •), and (iii) the liquid wedge (curves with ×). The dashed (solid) curves with symbols correspond to the centers $r = 0$, $x = 0$ (edges $r \approx R_L$, $x \approx R_L$) of the loaded area. In the case (i) the liquid pressure behind the shockwave is everywhere the same.

According to Fig. 3, for the small slope angles $\theta \leq 0.07$ the pressure values, computed by the technique of the present work in the case of impact by the liquid wedge, in the vicinity of the shockwave edge $x = R_L$ are in very good agreement with those, calculated by (5), behind the shockwave in the case of impact by the plane semi-infinite liquid flux. The influence of the axial symmetry manifests itself in only slightly reducing the wall pressure both in the center and at the edge of the loaded area.

4. Impact of a jet with hemispherical end on a liquid layer on a wall

Impact of an axisymmetric liquid ($\Gamma_1 = 7.15$, $B_1 = 3072$ bar) jet (surrounded by the air, $\gamma = 1.4$) with the hemispherical end on a rigid wall covered by a thin uniform layer of the same liquid is considered (Fig. 4*a*). Initially $\varphi = 1$, $\rho = 10^3$ kg/m^3 in the liquid, $\varphi = 0$, $\rho = 1$ kg/m^3, in the gas, and $p = 1$ bar everywhere. The jet velocity and radius are $V = 350$ m/s and $R = 10$ μm, the thickness of the liquid layer is equal to 0.04 R.

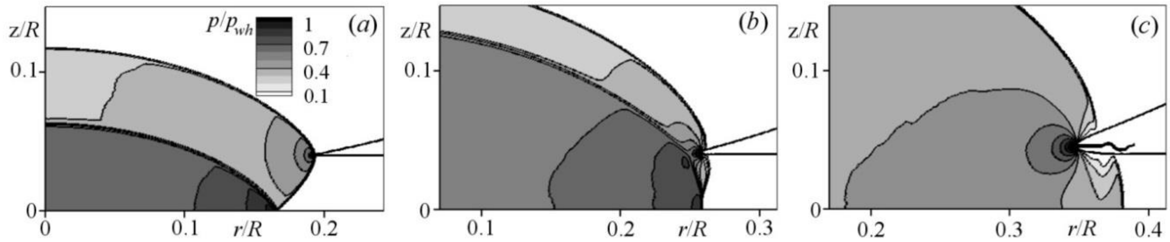

Figure 4. Impact of a liquid jet on a thin liquid layer on a wall: the gas-liquid interface, the fields of pressure in the half of the axial section in the vicinity of the jet end, p_{wh} = 7.7 kbar.

Liquid jet impact on a liquid layer on a wall results in appearance of two shockwaves, the pressure at the place of impact being approximately equal to half of the waterhammer pressure. One of the shockwaves propagates up the jet, while the other first moves in the layer to the wall and then reflects from it (Fig. 4*a*). Interaction of the second shockwave with the wall is divided into the stages of regular (Fig. 4*a*) and irregular (Fig. 4*b*) reflection. At the stage of regular reflection and in the beginning of the stage of irregular reflection the maximum pressure on the wall is attained at the edge of the reflection area. The levels of that maximum pressure are comparable with the waterhammer pressure. At the stage of irregular reflection the fronts of the oncoming and reflected shockwaves merge to produce the resultant shockwave in the vicinity of the wall. The resultant shockwave begins to propagate in the liquid layer and interact with its surface. The interaction leads to creation of a rarefaction wave which soon acts on the wall (Fig. 4*c*). A thin ring-like liquid splash arises in the space between the jet and the layer (Fig. 4*c*).

5. Conclusion

Main points of a numerical technique for computing problems of the high-speed liquid jet impact on a rigid wall are presented. In the technique, the liquid and gas flows are governed by the gas dynamics equations in the density, velocity and pressure. Their numerical integration is carried out by the CIP-CUP method with application of dynamically adaptive grids, the gas-liquid interface is calculated without explicit tracking.

To estimate the efficiency of the technique problems of impact on a wall of a liquid cone and a liquid wedge in the mode with the shockwave attached to the wall by their edges are considered. The pressure values computed by the presented technique are found to be in the vicinity of the edge of the shockwave attached to the wall in good agreement with the analytically determined pressure of the compressed liquid in a similar problem of impact on the pressure wall of a flat semi-infinite flux. The influence of the axial symmetry of the liquid cone impact on the liquid pressure in the vicinity of the shockwave edge is shown to be small.

Applicability of the presented technique to numerically simulating the high-speed liquid jet impact on a wall is illustrated by computing impact of a cylindrical liquid jet with the hemispherical end on a wall covered by a layer of the same liquid.

References

[1] Bowden F P and Brunton J H 1961 *Proc. R. Soc. Lond. A* **263** 433–50
[2] Bourne N K 2005 *Proc. R. Soc. Lond. A* **461** 1129–45
[3] Kornfeld M and Suvorov L 1944 *J. Appl. Phys.* **15** 495–506
[4] Hawker N A and Ventikos Y 2012 *J. Fluid Mech.* **701** 59–97
[5] Yabe T, Xiao F and Utsumi T 2001 *J. Comput. Phys.* **169** 556–93

[6] Yabe T and Wang PY 1991 *J. Phys. Soc. Japan* **60** 2105–08
[7] Abgrall R and Karni S 2001 *J. Comp. Phys.* 1**69** 594–623
[8] Takizawa K, Yabe T, Tsugawa Y, Tezduyar T E and Mizoe H 2007 *Comput. Mech.* **40** 167–83
[9] Heymann F J 1969 *J. Appl. Phys.* **40** 5113–22